Mon. Not. R. astr. Soc. (1991) **253**, 377–387

On the circular polarization in pulsar emission

A. Z. Kazbegi, G. Z. Machabeli and G. I. Melikidze
Abastumani Astrophysical Observatory, Kazbegi ave 2a, Tbilisi, Georgia Republic, 380060, USSR

Accepted 1991 June 26. Received 1991 June 24; in original form 1990 July 6

SUMMARY

A model explaining the existence and properties of the circular polarization in pulsar emission is offered. It is based on the properties of waves excited in pulsar magnetospheres by possible plasma instabilities. The cyclotron instability developing due to the anomalous Doppler effect is carefully investigated. The following characteristics of the emission polarization are explained: if circular polarization exists it should be confined to small angles and observed in the core-type emission; the maximum intensity of circular polarization in the profile window is near the intensity maximum of the core-type emission; the sense-reversals of circular polarization in some pulsars and their absence in others; the correlation between circular polarization and position-angle swings; the behaviour of circular polarization in PSR 1541 + 09, 1702 − 19 and others.

1 INTRODUCTION

Many pulsars emit radiation which is both linearly and circularly polarized, with the degree of circular polarization of the order of several per cent. Some pulsars, however, possess higher degrees of circular polarization (CP) – about 20 per cent (Manchester & Taylor 1977; Taylor & Stinebring 1986), up to 60 per cent in PSR 1702 − 19 (Biggs *et al.* 1988). There is, as yet, no satisfactory explanation of the CP and the aim of this paper is to propose a possible mechanism of generation of CP consistent with the theory of excitation of radio waves in pulsars. A spinning magnetized neutron star generates an electric field which extracts electrons from the star's surface and accelerates them to form a low-density ($n_b = 7 \times 10^{-2} B_0 P^{-1}$, where P is the pulsar period and B_0 the magnetic field at the star's surface) and energetic (the Lorentz factor of particles is $\gamma_b = 10^7$ for typical pulsars) primary beam. In a weakly curved magnetic field, electrons generate γ-quanta which in turn produce electron–positron pairs. The pitch angle of the particles which are produced is non-zero, so that secondary particles generate synchrotron radiation. This radiation in turn produces more pairs, and so on until the plasma becomes dense and screens the electric field (Goldreich & Julian 1969; Sturrock 1971). As a result a multicomponent plasma is formed, containing:

(i) electrons and positrons with $\gamma \sim \gamma_p$ and $n \sim n_p$;

(ii) a high-energy plasma 'tail' [the tail on the distribution function; see Fig. 1 which is from Arons (1981)] with $\gamma \sim \gamma_t$ and $n \sim n_t$;

(iii) the primary beam with $\gamma \sim \gamma_b$, $n \sim n_b$.

We assume equipartition of energy among the plasma components

$$n_p \gamma_p \approx n_t \gamma_t \approx \frac{n_b \gamma_b}{2}.$$

The total energy outflow of the particles can reach a value (Ruderman & Sutherland 1975)

$$L_{+-} \approx 10^{30} \left(\frac{B_0}{10^{12}\ \mathrm{G}}\right)^{6/7} \left(\frac{P}{1\ \mathrm{s}}\right)^{-15/7} \mathrm{erg\ s^{-1}}.$$

In the majority of papers devoted to the processes taking place in the relativistic electron–positron plasma, the distribution function of the electrons is assumed to be identical with that of the positrons, in which case the following components of the

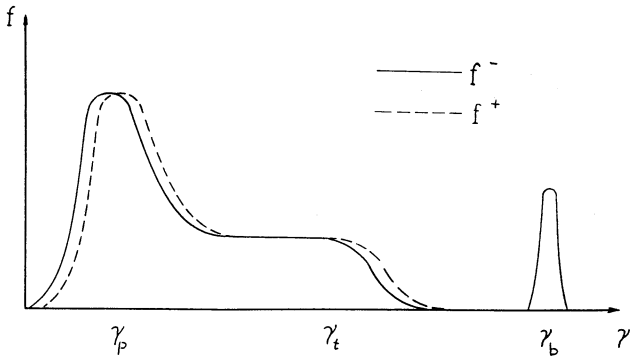

Figure 1. The one-dimensional distribution function of particles in the pulsar magnetosphere. f^- corresponds to the electron distribution function, f^+ to the positron one.

permittivity tensor $\varepsilon_{xy}=\varepsilon_{yx}=\varepsilon_{zy}=\varepsilon_{yz}$ equal zero (Volokitin, Krasnoselaskikh & Machabeli 1985; Lominadze *et al.* 1986). The waves propagating in such a plasma are only linearly polarized. In fact the distribution functions of electrons F^- and positrons F^+ are shifted with respect to each other (Fig. 1) due to the presence of the primary electron beam and the quasi-neutrality of the plasma as a whole. The value

$$\Delta\gamma=\gamma_+-\gamma_-=\int F^+\gamma d\boldsymbol{p}-\int F^-\gamma d\boldsymbol{p},\qquad \int F^{\pm}d\boldsymbol{p}=1, \tag{1}$$

determines the difference in energies of electrons and positrons. The value of $\Delta\gamma$ is small but of decisive significance in explaining the polarization properties of pulsars.

We introduce cylindrical coordinates x, r, φ to describe the curvature of magnetic field lines. The x-axis is transverse to the plane where the curved field line lies, r is the radial and φ the azimuthal coordinate. The latter describes the curvature of the field line (torsion is neglected and $\partial R_B/\partial \boldsymbol{r}=0$; R_B is the radius of curvature of the field line). In such a geometry one has the following integrals of motion: γ, $p_x-r\omega_{B\alpha}/c$, rp_φ. Here $p_i=v_i\gamma/c$ and v_i are the particle momentum and velocity, $\omega_{B\alpha}=e_\alpha B/mc$. The particle distribution function should depend on the integrals of motion. By integration along the particle trajectory, one obtains the components of the permittivity tensor:

$$\varepsilon_{xx}=1-\frac{1}{2}\sum_\alpha\frac{\omega_{p\alpha}^2}{\omega^2}\int\frac{dp_\varphi}{\gamma}\left[(\omega-k_\varphi v_\varphi-2k_\varphi u_\alpha^2/c)A_\alpha^+f_\alpha+2\omega\frac{u_\alpha^2}{c^2}\frac{\gamma}{\Omega_\alpha^0}\frac{\partial f_\alpha}{\partial\gamma}\right],$$

$$\varepsilon_{rr}=1-\frac{1}{2}\sum_\alpha\frac{\omega_{p\alpha}^2}{\omega^2}\int\frac{dp_\varphi}{\gamma}(\omega-k_\varphi v_\varphi-k_x u_\alpha)A_\alpha^+f_\alpha,\qquad \varepsilon_{\varphi\varphi}=1+\sum_\alpha\frac{\omega_{p\alpha}^2}{\omega}\int dp_\varphi\frac{v_\varphi^2}{c^2\Omega_\alpha^0}\frac{\partial f_\alpha}{\partial\gamma},$$

$$\varepsilon_{xr}=-\frac{i}{2}\sum_\alpha\frac{\omega_{p\alpha}^2}{\omega^2}\int\frac{dp_\varphi}{\gamma}(\omega-k_\varphi v_\varphi-k_x u_\alpha)A_\alpha^-f_\alpha,\qquad \varepsilon_{rx}=\frac{i}{2}\sum_\alpha\frac{\omega_{p\alpha}^2}{\omega^2}\int\frac{dp_\varphi}{\gamma}(\omega-k_\varphi v_\varphi-2k_\varphi u_\alpha^2/c)A_\alpha^-f_\alpha,$$

$$\varepsilon_{x\varphi}=-\frac{1}{2}\sum_\alpha\frac{\omega_{p\alpha}^2}{\omega^2 c}\int\frac{dp_\varphi}{\gamma}v_\varphi\left[(k_xcA_\alpha^++ik_rcA_\alpha^-)f_\alpha+2\omega\frac{u_\alpha}{c}\frac{\gamma}{\Omega_\alpha^0}\frac{\partial f_\alpha}{\partial\gamma}\right],$$

$$\varepsilon_{\varphi x}=-\frac{1}{2}\sum_\alpha\frac{\omega_{p\alpha}^2}{\omega^2 c}\int\frac{dp_\varphi}{\gamma}v_\varphi\left\{[(k_xc-2k_\varphi u_\alpha)A_\alpha^+-ik_rcA_\alpha^-]f_\alpha+2\omega\frac{u_\alpha}{c}\frac{\gamma}{\Omega_\alpha^0}\frac{\partial f_\alpha}{\partial\gamma}\right\},$$

$$\varepsilon_{r\varphi}=-\frac{1}{2}\sum_\alpha\frac{\omega_{p\alpha}^2}{\omega^2 c}\int\frac{dp_\varphi}{\gamma}v_\varphi\{[k_rcA_\alpha^+-i(k_xc-2k_\varphi u_\alpha)A_\alpha^-]f_\alpha\},\qquad \varepsilon_{\varphi r}=-\frac{1}{2}\sum_\alpha\frac{\omega_{p\alpha}^2}{\omega^2 c}\int\frac{dp_\varphi}{\gamma}v_\varphi\{[k_rcA_\alpha^++i(k_xc-2k_\varphi u_\alpha)A_\alpha^-]f_\alpha\}. \tag{2}$$

Here ,

$$A_\alpha^+ = \left(\frac{1}{\Omega_\alpha^+} + \frac{1}{\Omega_\alpha^-}\right), \qquad A_\alpha^- = \left(\frac{1}{\Omega_\alpha^-} - \frac{1}{\Omega_\alpha^+}\right), \qquad \Omega_\alpha^\pm = \omega - k_\varphi v_\varphi - k_x u_\alpha \pm \omega_{B\alpha}\gamma^{-1}, \qquad \Omega_\alpha^0 = \omega - k_\varphi v_\varphi - k_x u_\alpha,$$

$$\omega_{p\alpha}^2 = 4\pi e^2 n_{p\alpha}/m, \qquad f_\alpha = \int dp_\perp p_\perp F_\alpha;$$

F is the particle distribution function; $p_\perp = \sqrt{p_r^2 + (p_x - u\gamma/c)^2}$; the sum over α is taken over the particle species [(i) electrons and positrons of the bulk of plasma, (ii) electrons and positrons of the 'tail', (iii) electrons of the primary beam] and the integration from $-\infty$ to $+\infty$; and $u_\alpha = v_\varphi p_\varphi c/\omega_{B\alpha} R_B$ is the particle drift velocity caused by the weak inhomogeneity of the magnetic field and directed along the x-axis for positrons (hereafter, for values without the subscript α, the sign of the charge is assumed to be positive). For the particles of the bulk of plasma the drift velocity u tends to zero. Hence, if one assumes $u_\alpha = 0$, equation (2) reduces to the standard form which we designate as ε_{ij}^p. Thus $\varepsilon_{ij} = \varepsilon_{ij}^p + \varepsilon_{ij}^r$, where ε_{ij}^r describes the contribution of the tail and the beam in the permittivity tensor. $|\varepsilon_{ij}^r| \ll |\varepsilon_{ij}^p|$ everywhere except in the resonance region.

2 POLARIZATION OF WAVES PROPAGATING IN PULSAR MAGNETOSPHERE

Let us investigate the polarization of waves propagating in the magnetospheric plasma. For this purpose it is convenient to take Maxwell's equations in the reference frame where the z'-axis is directed along $\boldsymbol{k}$:

$$\left[(k'^2\delta_{lm} - k'_l k'_m)\frac{c^2}{\omega^2} - \varepsilon_{lm}^{p'}\right] E'_m = 0, \tag{3}$$

where E'_m are components of the wave electric vector, $l, m = (x', y', z')$.

From expressions (2) it follows that the curvature does not affect ε_{ij}^p. Thus the Cartesian coordinate system (x, y, z) can be used with the z-axis directed along the tangent to the magnetic field line. The direction of the $\boldsymbol{k}$ vector (the z'-axis) is arbitrary and it makes angle θ with the z-axis and angle Ψ with the zOy plane (Fig. 2). By rotation about the Ψ angle, the y'- and y-axes can be made to match. By rotation about the θ angle, both coordinate systems coincide. If one introduces the following designations, $\alpha_x = E'_x/iE'_y$ and $\alpha_z = E'_z/iE'_y$, i.e. $\boldsymbol{E}' = E'_y(i\alpha_x; 1; i\alpha_z)$, then, by using the relations connecting the values taken in the system x, y, z with those in the x', y', x' system, one obtains from equation (3) (Shafranov 1967)

$$\alpha_x^2 - \frac{\eta_{xx} - \eta_{yy}}{i\eta_{yx}}\alpha_x - 1 = 0 \tag{4}$$

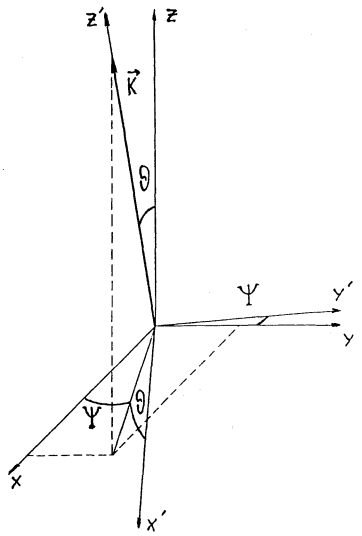

Figure 2. The position in space of two Cartesian coordinate systems x', y', z' and x, y, z with respect to each other. θ is the angle between the z-axis and $\boldsymbol{k}$ (the z'-axis). Ψ is the angle between the $\boldsymbol{k}$-vector projection on the xOy plane and the x-axis.

where

$$\eta_{xx}=\varepsilon^{p'}_{xx}-\frac{\varepsilon^{p'}_{xz}\varepsilon^{p'}_{zx}}{\varepsilon^{p'}_{zz}},\qquad \eta_{yx}=-\varepsilon^{p'}_{yx}+\frac{\varepsilon^{p'}_{yz}\varepsilon^{p'}_{zx}}{\varepsilon^{p'}_{zz}},\qquad \eta_{yy}=\varepsilon^{p'}_{yy}-\frac{\varepsilon^{p'}_{yz}\varepsilon^{p'}_{zy}}{\varepsilon^{p'}_{zz}}. \tag{5}$$

The solution of equation (4) is

$$\alpha_x=\frac{1}{2}\frac{\eta_{xx}-\eta_{yy}}{i\eta_{yx}}\pm\left[\frac{1}{4}\left(\frac{\eta_{xx}-\eta_{yy}}{\eta_{yx}}\right)^2+1\right]^{1/2}. \tag{6}$$

We shall be interested only in waves propagating in the observer's direction. Because of relativistic compression, the angle between the local magnetic field $\boldsymbol{B}$ and the wavevector $\boldsymbol{k}$ is small, $\theta^2=(k_\perp/k_z)^2\ll 1$. Using the determination of ε^p_{ij}, formulae (2) and (6) and expanding in a series of small parameters $\theta^2\ll 1$, $\Delta\gamma/\gamma<1$, $\omega_p^2/\omega_B^2\ll 1$, we obtain

$$\frac{1}{2}\frac{\eta_{xx}-\eta_{yy}}{i\eta_{yx}}=-\frac{4\theta^2\omega_B\gamma_p^4}{\omega\Delta\gamma}\equiv a,$$

where γ_p is the average Lorentz factor of the bulk of plasma.

If

$$\theta^2\gg\left(\frac{\omega}{4\omega_B}\right)\frac{\Delta\gamma}{\gamma_p^4}\qquad\text{and}\qquad a\gg 1 \tag{7}$$

it follows from equation (6) that there are two linearly polarized waves in the relativistic electron–positron plasma:

$$\alpha_x\ll 1\quad\text{or}\quad\alpha_x\gg 1.$$

The first mode has the prevailing component E'_y, i.e. the vector of the electric field $\boldsymbol{E}'$ lies in the plane of $\boldsymbol{k}$ and $\boldsymbol{B}$. This is a mixed potential–non-potential lt-wave (see e.g. Volokitin *et al.* 1985). The electric vector E'_x of the second wave is transverse to the plane of $\boldsymbol{k}$ and $\boldsymbol{B}$, and the wave is called a transverse t-wave.

In the opposite case, when

$$\theta^2\ll\frac{\omega\Delta\gamma}{4\omega_B\gamma_p^4}, \tag{8}$$

one obtains two CP waves

$$\alpha_x=\pm 1$$

with left-handed (in the direction of electron rotation) and right-handed (in the direction of positron rotation) polarization. The intermediate cases have elliptical polarization since generally $E=E_x+iE_y$.

A similar problem was investigated by Allen & Melrose (1982). Their result is given by the equations

$$\frac{2g}{a-b}=\begin{cases}\ll 1-\text{the polarization is linear}\\ \gg 1-\text{the polarization is circular,}\end{cases}$$

where

$$a-b=-\sum_\alpha\left(\frac{4\omega_{p\alpha}^2}{\omega^2}\right)\int_1^\infty\frac{\gamma\theta^2 f(\gamma)}{1+\gamma^2\theta^2}\,d\gamma,\qquad g=-\sum_\alpha\frac{\omega_{p\alpha}^2}{2\omega\omega_B}\int_1^\infty\frac{(1-\gamma^2\theta^2)\,f(\gamma)}{\gamma^2}\,d\gamma.$$

Note that the expression for g is valid only when one neglects all terms except ω_B/γ in the denominator under the integral $\Omega_\alpha^\pm=\omega-k_\varphi v_\varphi-k_x u_\alpha\pm\omega_{B\alpha}/\gamma$. Neglecting u_α (for plasma particles it is almost zero) and using (11) (see below) for the spectrum of waves, one finds that it is valid only if $\theta^2\ll 2\omega_B/\omega\gamma$. After summing over the particle species it can be seen that the second term in the expression for g vanishes,

$$\int_1^\infty(f^+\,d\gamma-f^-\,d\gamma)=n^+-n^-=0,$$

and the first term yields

$$g=-\frac{\omega_p^2}{2\omega\omega_B}\left(\frac{1}{\gamma_+^2}-\frac{1}{\gamma_-^2}\right)=-\frac{\omega_p^2}{\omega\omega_B}\frac{\Delta\gamma}{\gamma^3}.$$

Thus the result differs from that of Allen & Melrose (1982) [their equations (13), (13′)]; in particular, for $\gamma^2\theta^2\gg 1$ one obtains $2g/(a-b)=\theta^2\Delta\gamma\omega/4\omega_B$. For CP to originate they need $\theta^2\gg 4\omega_B/\Delta\gamma\omega$, which contradicts the approximation $\theta^2\ll 2\omega_B/\omega\gamma$ above. For small angles ($\theta^2\ll\gamma^{-2}$) the condition for θ coincides with equation (8). Hence CP waves can be obtained only for small angles θ (equation 8). Evidently the existence of CP cannot be explained by an increase of θ after propagation of a linearly polarized wave in a plasma (e.g. Allen & Melrose 1982; Radhakrishnan & Rankin 1990).

3 WAVE GENERATION AND PROPAGATION

In our opinion the maser emission mechanisms (Ginzburg & Zheleznyakov 1975) are the only well-grounded ones (compared with others such as antenna mechanisms; for more details see Lominadze *et al.* 1986). We give below additional arguments confirming this opinion.

The excited waves propagate in the magnetospheric plasma, leave it and reach the observer preserving all their properties while crossing the plasma–vacuum boundary (Lominadze et al. 1986). We shall treat only waves having $\theta^2\ll 1$ and $k_\perp v_\perp/\omega_B\ll 1$, $v_\perp=p_\perp c/\gamma$, but the dispersion relation following from (2) is nevertheless very complicated. However, as mentioned above, the spectrum of the waves is determined by ε_{ij}^p. In this case the dispersion relation splits into three equations:

$$\varepsilon_{\varphi\varphi}^p=0, \tag{9}$$

$$\frac{k^2c^2}{\omega^2}=\varepsilon_{xx}^p\pm i\varepsilon_{rx}^p. \tag{10}$$

Equation (9) describes purely potential (longitudinal) waves with $\alpha_z\gg 1$, and we shall not be concerned with them further. The real parts of frequency $\omega_0\equiv\mathrm{Re}\,\omega$ calculated for the two equations (10) [i.e. for both signs of equation (10)] do not resemble each other and yield the spectrum of t-waves (*cf.* Machabeli & Usov 1979):

$$\omega_0=kc\left(1-\frac{1}{4}\frac{\omega_p^2}{\omega_B^2}\frac{1}{\gamma_p^3}\right)\equiv kc(1-\delta). \tag{11}$$

Let us investigate the possibility of t-wave generation at the cyclotron resonance (see equation 2):

$$\omega_0-k_\varphi v_\varphi-k_x u_a\pm\frac{\omega_{Ba}}{\gamma}=0. \tag{12}$$

Substituting (11) and the expressions $k=k_\varphi(1+k_\perp^2/2k_\varphi^2)$ and $v_\varphi=c(1-1/2\gamma^2-u^2/2c^2)$ in (12), one obtains

$$\frac{k_r^2}{2k_\varphi^2}+\frac{1}{2\gamma_{\mathrm{res}}^2}+\frac{1}{2}\left(\frac{k_x}{k_\varphi}-\frac{u_a}{c}\right)^2-\delta=\mp\frac{\omega_B}{k_\varphi c\gamma_{\mathrm{res}}}. \tag{13}$$

As was shown by Machabeli & Usov (1979), t-waves are excited in the pulsar magnetosphere only by the anomalous Doppler effect [upper sign of equation (13)]. The lower sign of (13) corresponds to wave damping. In the plasma rest frame (the frame moving along $\boldsymbol{B}_0$ with $\gamma=\gamma_p$ relative to the laboratory one), these conditions are fulfilled for velocities satisfying the condition (Lominadze *et al.* 1986)

$$\frac{v'}{c}=\frac{\omega_0'k_\varphi'v_\varphi'\pm|\omega_B|\sqrt{\omega_B^2+k_\varphi'^2v_\varphi'^2-\omega_0'^2}}{\omega_B^2+k_\varphi'v_\varphi'^2}. \tag{14}$$

It is obvious that, for the whole range of frequencies $\omega_0'=k'c<\omega_B$, damping [lower sign in (14)] can occur only for particles having negative velocities, so, for the distribution function given in Fig. 1, damping is absent at $\omega\ll\omega_B$. In the case when the resonant condition $\omega_0-k_\varphi v_\varphi-k_x u-\omega_B/\gamma=0$ is nevertheless fulfilled, waves are strongly damped and cannot reach an observer. Thus the existence of CP cannot be explained by propagation effects (Cheng & Ruderman 1977; Beskin, Gurevich & Istomin 1988).

Hence, for energetic particles, only the resonance due to the anomalous Doppler effect [upper sign of (13)] can be satisfied. Therefore, taking into account the resonant part of the ε_{ij}, one obtains the following dispersion relation for t-waves:

$$\frac{k^2c^2}{\omega^2} = \varepsilon_{xx}^{p} \pm i\varepsilon_{rx}^{p} - (\varepsilon_1^{\pm} + \varepsilon_2^{\pm}), \tag{15}$$

where

$$\varepsilon_1^{\pm} = \frac{\omega_{p\,\mathrm{res}}^2}{2\omega^2}\int \frac{f^{\pm}(\omega - k_\varphi v_\varphi - 2k_\varphi u^2/c)\,dp_\varphi}{\gamma(\omega - k_\varphi v_\varphi \mp k_x u + \omega_B/\gamma)}, \qquad \varepsilon_2^{\pm} = \frac{\omega_{p\,\mathrm{res}}^2}{2\omega^2}\int \frac{f^{\pm}(\omega - k_\varphi v_\varphi \mp k_x u)\,dp_\varphi}{\gamma(\omega - k_\varphi v_\varphi \mp k_x u + \omega_B/\gamma)}.$$

The growth rate of cyclotron instability is

$$\Gamma = \pi\frac{\omega_{p\,\mathrm{res}}^2}{\omega_0\gamma_{\mathrm{T}}} \quad \text{if} \quad \frac{1}{2}\frac{u^2}{c^2} \ll \delta \tag{16}$$

and

$$\Gamma = \pi\frac{\omega_{p\,\mathrm{res}}^2}{2\omega_0\gamma_{\mathrm{T}}}\frac{u^2}{\delta c^2} \quad \text{if} \quad \frac{1}{2}\frac{u^2}{c^2} \gg \delta, \tag{17}$$

where the resonant frequency is defined as $\omega_0 \approx \omega_B/\delta\gamma_{\mathrm{res}}$ (γ_{T} and γ_{res} are the thermal spread and the average Lorentz factor of the resonant particles respectively). The damping of t-waves is due to the particles of the bulk of plasma; the corresponding decrement is given by

$$\Gamma' = -\pi\frac{\omega_p^2}{\omega_0\gamma_p}, \tag{18}$$

and the frequency of damped waves is $\omega_0 \approx 2\gamma_p\omega_B$. The solution of the first equation (15) (the upper signs) yields wave generation by resonant electrons (left-handed CP) and damping by plasma positrons, while for the second one (lower signs) there is wave generation by positrons (right-handed CP) and damping by electrons. However, as was already mentioned above, damping for the distribution function given in Fig. 1 and at $\omega_0 \ll 2\gamma_p\omega_B$ is absent.

Let us consider the resonant condition (13) in detail. This condition is satisfied only if $1/2\gamma_{\mathrm{res}}^2 < \delta$. This is possible if the resonance arises for the particles in both the tail of the distribution function and the primary beam (Fig. 1). The expression (16) is satisfied only under certain conditions. The following is true for the dipole magnetosphere where $\omega_B = \omega_{B_0}(R_0/R)^3$ and $\omega_p = \omega_{p_0}(R_0/R)^{3/2}$ (R_0 is the pulsar radius, ω_{B_0} and ω_{p_0} are gyro and plasma frequencies at the stellar surface). For the parameters of typical pulsars ($P = 1$ s) (Arons 1981), expression (13) is fulfilled at distances 10^9 cm $\leq R \leq 5\times10^9$ cm in a limited region, the width of which is 10^7–10^8 cm (Kazbegi, Machabeli & Melikidze 1987). Note that there is no restriction on the value $\theta^2 \equiv (k_\perp/k_\varphi)^2$ from below. Therefore, on emergence from the pulsar magnetosphere there will be an entire circle filled with radiation (from the cone intersection) and thus emission of 'core' type.

There is a problem of wave escape from the magnetospheric plasma, which is a problem for any pulsar model. The waves emerge from the generation region having an angle θ with respect to the magnetic field lines and propagate through the dense plasma in the direction of decreasing magnetic field. Eventually they reach the region of cyclotron absorption. Note that the magnetic field is 'frozen' in the plasma. Particles move relativistically along the field lines and at the same time they corotate with the star and frozen-in field lines. Approaching the light cylinder, the mass of particles increases due to relativistic effects and as a result all field lines bend in one direction. We suppose that our wave generation region is located near the boundary between the open and closed field lines. In such a case the waves find themselves in regions with low plasma density and escape into the interstellar medium without transformation (Fig. 3).

Three possible wave-generation mechanisms are considered by Kazbegi *et al.* (1989a) (apparently there is no other possibility of wave generation in the stationary plasma of a pulsar magnetosphere). Two of them occur at distances of the order of $R \geq 10^9$ cm from the neutron star, as the resonances $\omega - k_\varphi v_\varphi = 0$ and $\omega - k_\varphi v_\varphi - k_x u = 0$ occur. For these mechanisms the angles θ_1 and θ_2 are restricted both from above and from below. Therefore the intersection of the emission diagram has the form of a ring of definite thickness. We believe that this is the emission of 'cone-type'. In Kazbegi, Machabeli & Melikidze (1989b), it is shown that the angles of waves excited by different mechanisms satisfy the inequality $\theta^{\mathrm{core}} < \theta_1^{\mathrm{cone}} < \theta_2^{\mathrm{cone}}$. Hence the emission diagram can be presented as the intersection of three cones put in each other (Kazbegi *et al.* 1989b).

The conditions for generation of cone-type emission are very strict and even a slight change of the magnetospheric parameters will break them. Generation of cone-type emission takes place by the Cherenkov-type resonance if the angles θ_1 or

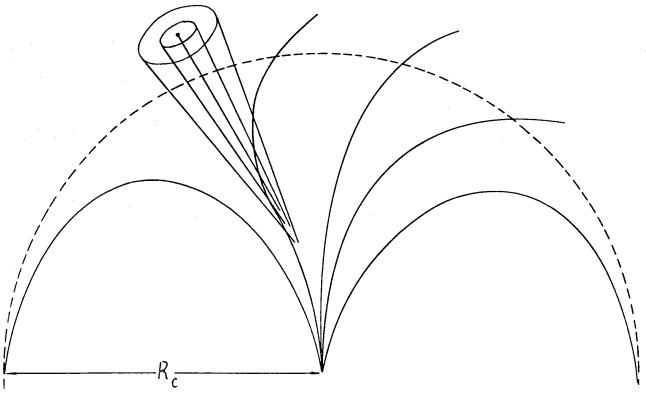

Figure 3. A schematic picture of the radiation region and the cross-section of the radiation pattern.

θ_2 are sufficiently large. Hence, in this case, waves with CP cannot be generated. Consequently the high degrees of CP can be found only in profiles with core-type emission. The same conclusion is reached by analysis of average profiles from observational data (Radhakrishnan & Rankin 1990).

The polarization theory above describes individual pulses. However, as is shown by Backer & Rankin (1980), the CP in individual pulses is observed not only in core components but in conal ones also. Note that, in our case, t- and lt-waves can be excited simultaneously in cone-type emission. Due to the difference of propagation velocities, the waves will reach an observer with definite phase shift that will remain unchanged for a definite time. An observer equipped with a crossed-dipole receiver will interpret the radiation as elliptically polarized. Over the pulse window an observer will detect waves coming from different field lines. Hence, in each individual pulse, the sign and intensity of CP will be variable as is also found from observations (Ferguson & Seiradakis 1978). Moreover, when detecting subsequent individual pulses, the place and polarization of subpulses should vary due to slight changes of plasma parameters. Let us call a wave having intrinsic CP a 'true' CP wave. This wave should differ from one constructed from two orthogonally polarized modes (t and lt). Summation of the latter over many pulses should cause the total amount of CP to vanish due to its random fluctuations, whereas integration of a true CP wave should give the total amount of CP with definite sign and intensity. Thus, in integrated profiles we should observe almost zero CP in conal components (wings of the profile) and CP emission in core components. We shall consider below only the true CP waves.

4 INTERPRETATION OF THE OBSERVATIONAL DATA

The theory presented here should explain the main properties of pulsar radiation, in particular the following (Rankin 1983, 1986; Lyne & Manchester 1988; Radhakrishnan & Rankin 1990).

(1) The existence of low to moderate amounts of CP in core-type emission, and a high degree of non-polarized emission in some pulsars.

(2) The fact that the intensity maximum of CP in average profiles is mainly in the centre of the pulse; the decrease of CP intensity to minimum at minimal impact parameters.

(3) The sense-reversal of CP (antisymmetric CP) in some pulsars and not (symmetric CP) in others. Two sense-reversals within a pulse window observed in very few pulsars (virtually only PSR 1541 + 09 provides a good example).

(4) Correlation of antisymmetric CP with linear polarization. A transition $+/-$ (changing of left-handed to right-handed polarization) is accompanied by a decrease of the linear polarization position angle (PA), while for transitions $-/+$ the PA increases.

(5) A high percentage of CP is PSR 1702 − 19 (60 per cent) and one sense of CP in both the main pulse and the interpulse.

We shall show below that all these properties can be explained within the framework of our theory without any additional assumptions.

The larger $\theta^2 \equiv (k_\perp/k_\varphi)^2$ is, the better the condition (7) $\theta^2 \gg \Delta\gamma k_\varphi c/4\gamma_p^4\omega_B$ is fulfilled, i.e. when the sight line cuts the emission diagram as far as possible from the diameter (large impact parameter). In this case the emission must be characterized by the two linearly polarized orthogonal t- and lt-modes $(\boldsymbol{E}_t \cdot \boldsymbol{E}_{lt}) = 0$ (Kazbegi *et al.* 1989a). The transitions between the two modes are described elsewhere (Kazbegi *et al.* 1989b). According to this paper the transitions are accompanied by a change of dominance between core- and cone-type emissions. The conclusion drawn by Stinebring *et al.* (1984) is similar to ours.

If $\Delta\gamma$ is so small that the inequality (7) is fulfilled even for small angles ($\theta^2 \ll 1$), we have only linearly polarized modes. The electric vector of t-waves is transverse to the plane of $\boldsymbol{k}$ and $\boldsymbol{B}_0$, whereas the vector $\boldsymbol{E}_{lt}$ lies in the $\boldsymbol{k}$ and $\boldsymbol{B}_0$ plane. For minimal values of $k_\perp$ (in the pulse window centre), $\boldsymbol{k}$ is almost parallel to $\boldsymbol{B}_0$. The plane of $\boldsymbol{k}$ and $\boldsymbol{B}_0$ turns into a line. Consequently it is

impossible to distinguish between t- and lt-modes, and the orientation of $\boldsymbol{E}_t$ in the plane perpendicular to $\boldsymbol{B}_0$ is arbitrary. The observed emission is unpolarized and again zero CP should be observed.

If the sight line cuts the cone of core-type emission near the diameter, then, in the centre of the pulse window, waves having small θ (in our model the smallness of θ corresponds to the smallness of the impact parameter) are observed. In this case there is a good possibility for the condition (8) $\theta^2 \ll \Delta\gamma k_\varphi c/4\gamma_p^4\omega_B$ to be fulfilled. Then, as follows from (6), $\alpha_x = \pm 1$ and there are two circularly polarized waves. The expressions (16, 17) lead to the possibility of wave generation both by electrons and positrons. Electrons produce the left-handed (+) and positrons the right-handed (−) polarization. However, the waves are excited only if equation (13) with upper sign is satisfied, and this is only when

$$\delta = \frac{\omega_B}{k_\varphi c\gamma_{\rm res}} + \frac{1}{2}\left(\frac{k_x}{k_\varphi} - \frac{u_\alpha}{c}\right)^2 + \frac{1}{2}\frac{k_r^2}{k_\varphi^2}. \tag{19}$$

Here we assume that $\delta \gg 1/\gamma_{\rm res}$. The condition (19) can be met in two cases. First, when

$$2\delta > \max\left[\left(\frac{k_\perp}{k_\varphi}\right)^2; \left(\frac{u}{c}\right)^2\right], \tag{A}$$

the condition (19) is satisfied for both species of particles (electrons and positrons), which excite waves with the growth rate (16).

Secondly, if

$$\frac{k_r^2}{k_\varphi^2} \ll 2\delta \leq \left[\left(\frac{k_x}{k_\varphi}\right)^2; \left(\frac{u}{c}\right)^2\right], \tag{B}$$

the corresponding growth rate is given by (17). The drift velocity $\boldsymbol{u}$ is directed perpendicular to the plane where the curved field line lies. To satisfy (19) the additional strict condition $k_x/k_\varphi = u_\alpha/c$ is necessary.

Let us consider the latter first. As we have already seen, the open magnetic field lines are almost parallel to each other. This means that one can choose the plane of field lines as the $r\varphi$ plane. As the field lines are parallel to each other, $\boldsymbol{u}$ does not change its orientation, whereas the wavevector $\boldsymbol{k}$ changes as the sight line cuts the emission cone. One observes the succession of $\boldsymbol{k}$ located along the cone. The condition

$$\left(\frac{k_x}{k_\varphi} - \frac{u_\alpha}{c}\right)^2 \equiv \frac{k_x^2}{k^2} + \frac{u^2}{c^2} - 2\frac{k_\perp}{k_\varphi}\frac{u_\alpha}{c}\cos\psi = 0$$

is fulfilled only if $k_\perp u_\alpha \cos\psi > 0$. The sight line can cut the emission cone in such a way that the angle ψ passes through phase $\pi/2$, so the sign of $\cos\psi$ changes. For the value $k_\perp u_\alpha \cos\psi$ to remain positive, it is necessary to change the sign of the drift velocity (the drift caused by the magnetic field inhomogeneity forces electrons and positrons to drift in opposite directions); i.e. for the angles $-\pi/2 < \psi < \pi/2$, the resonant condition (19) is fulfilled for positrons (right-handed CP); and, for $\pi/2 < \psi < 3\pi/2$, for electrons (left-handed CP). Hence, cutting of the sight line of the emission cone in a place where ψ changes its phase (near $\psi \approx \pi/2$) is accompanied by a change of the sense of CP. Such changes are observed for PSR 1237+25, 1839+09, 1907+03 and others (for details see Radhakrishnan & Rankin 1990). If $\psi \to \pi/2$, $\cos\psi \to 0$ and the resonance (19) breaks, because $(k_x/k_\varphi - u_\alpha/c)^2 > \delta$. Hence, when the sight line passes phase $\pi/2$, the degree of CP intensity decreases.

Let us return to the case (A). Then both species of particles satisfy the condition (19). Thus the intensity of CP emission should be considerably reduced, because it is proportional to the difference in numbers of resonant electrons and positrons. But, according to Fig. 1, we have more positrons in the resonant region. Hence waves are excited having right-handed CP with reduced intensity. If the distribution functions coincide ($\Delta\gamma = 0$), two modes of CP superpose giving two linearly polarized waves with electrical vectors orthogonal. As was shown, they can give rise to non-polarized emission if $k_\perp \to 0$.

The spectrum of excited t-waves is given by (11) and the resonant frequency is $\omega_0 = \omega_B/\delta\gamma_{\rm res}$. In the dipole magnetosphere one can assume that $B = B_0(R_0/R)^3$ and $n = n_0(R_0/R)^3$, where the index 0 denotes the values taken at the stellar surface. Using these expressions one obtains

$$\omega_0 = {\rm const}\left(\frac{R_0}{R}\right)^6.$$

It is evident that we have the well-known case of radius-to-frequency mapping, the lower the frequency the higher being the distance to the generation region.

At the same time $\delta = \delta_0(R/R_0)^3$ and $(u/c) = (u_0/c)(R/R_0)^2$. The comparison of these values shows that, at distances $R < 2\times 10^9$ cm, $(u/c)^2 < \delta$, and, for $R > 2\text{–}3\times 10^9$ cm, $\delta < (u/c)^2$ (all calculations are carried out for typical pulsars). Thus the

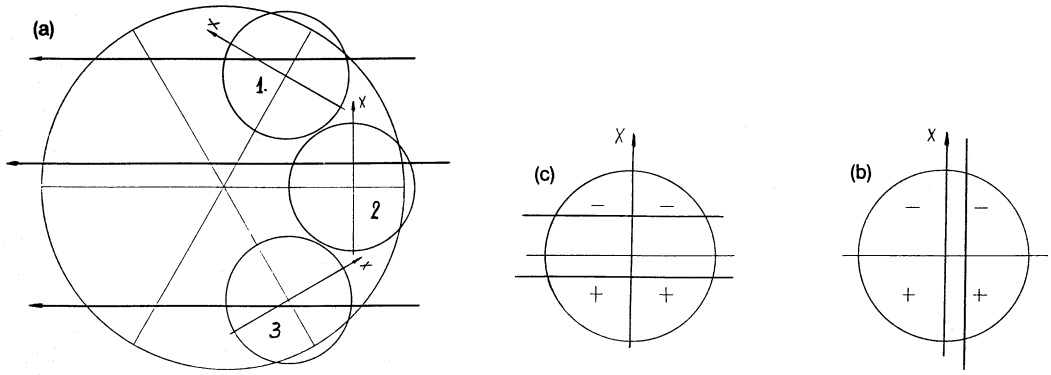

Figure 4. (a) The projection on to the polar cap. Small circles (regions 1, 2 and 3) are the radiation cones. The solid lines represent different sight-line trajectories (different impact parameters). (b) The cross-section of the core-type radiation pattern in the case (B). The solid line represents the direction of the sight line. The CP changes as $-/+$ when the sight line crosses the cone from top to bottom (region 3), and as $+/-$ when the sight line crosses the cone from bottom to top (region 1). (c) The cross-section of the core-type radiation pattern in case (A). The CP is symmetric (region 2).

possibility for CP to change its sense [i.e. when $\delta < (u/c)^2$] is higher at larger distances, $R > 2\text{–}3 \times 10^9$ cm, hence at lower frequencies.

The wave generation occurs at distances $R > 10^9$ cm. Thus two regions can be considered. The first, where the rotating pulsar bends the magnetic lines in a direction opposite to the rotation, is at distances about $R > 0.5R_c \approx 2.5 \times 10^9$ cm (for a typical pulsar) where R_c is the light cylinder radius. The field lines are in the plane perpendicular to the rotation axis $\boldsymbol{\Omega}$. The drift velocity is transverse to the plane where the curved field line lies, i.e. $\boldsymbol{u} \| \boldsymbol{\Omega}$. The sight line is always perpendicular to x-axis and the sign of $\cos\psi$ remains unchanged, so we have symmetric CP (Fig. 4c). The second region is located at $R < 0.5R_c \approx 2.5 \times 10^9$ cm where the field has dipolar structure. For different sight-line trajectories (with respect to the magnetic moment $\boldsymbol{\mu}$), the x-axis will make different angles to the plane of $\boldsymbol{\mu}$ and $\boldsymbol{\Omega}$ (this angle ζ varies from $-\pi/2$ to $\pi/2$) (Fig. 4a). At the same time the variation of ζ in each concrete emission cone is small; hence $\boldsymbol{u}$ will remain unchanged whereas the wavevector $\boldsymbol{k}$ changes as the sight line cuts the emission cone. One observes the succession of $\boldsymbol{k}$ located along the cone. If the condition (B) is met and the sight line cuts the magnetosphere so that β (the impact parameter) is small [region 2 on Fig. 4(a) – the corresponding ζ is near to zero], one should observe symmetric CP (Fig. 4c). If β is large, one should cut the region 1 or 3 (Fig. 4a) where $\zeta \approx \pi/2$. The sight line will be parallel to the x-axis and antisymmetric CP should be observed (with the $+/-$ transition in region 1 and $-/+$ transition in region 3) (Fig. 4b). If case (A) is met, the sign of CP remains unchanged for any value of β.

One of the predictions of such a model is the possibility of detecting a pulsar having symmetric CP at high frequencies [case (A) at $R < 0.5R_c$], antisymmetric CP at moderate frequencies [case (B) at $R < 0.5R_c$], and again symmetric CP at low frequencies [case (B) at $R > 0.5\,R_c$]. The intensity of symmetric CP at low frequencies should be more than that at high frequencies.

Let us investigate the behaviour of the PA within the framework of the theory suggested. In the core-type components, for small angles $\theta^2 \ll 1$ only t-waves are excited with $\boldsymbol{E}_t \perp \boldsymbol{k}$ (Kazbegi *et al.* 1989a). The variation of the $\boldsymbol{E}_t$ direction is described by the rotation of the position angle χ. The χ-angle is counted off from the point $\psi = \pi/2$.

Fig. 5 represents possible trajectories of sight lines and the corresponding changes in the direction of the vector $\boldsymbol{E}_t$. The PA swing across the pulse is attributed to the changing direction of the electric field $\boldsymbol{E}_t$. One can see the correlation between the sense-reversing CP and the direction of the PA rotation. At the $+/-$ transition the PA decreases, and vice versa (Fig. 5).

PSR 1542+09 changes its handedness twice $+/-/+$ (from left-handed to right one and again left) (Rankin, Stinebring & Weisberg 1989). When can it take place? Let us return to the resonance condition (19). It can be satisfied only in two cases: (A) and (B) accompanied by the additional condition $k_x^2/k_\varphi^2 + u^2/c^2 - 2k_\perp u_\alpha \cos\psi/k_\varphi c = 0$. The latter is satisfied better, the closer the value of $\cos\psi$ is to 1, i.e. at angles $\psi \approx 0;\ \pi$. Consider that the generation region is located at that pole where electrons rotate clockwise and produce a right-hand polarized wave $(-)$. The direction of the x-axis that is along the direction of positron drift changes to the opposite, due to the fact that, as $\boldsymbol{B}_0 \to -\boldsymbol{B}_0$, positrons change their drift direction to the opposite. Then, in case (A) the wave is generated with left-handed polarization $(+)$ due to greater number of positrons in the generation region. Let us consider the sight line along which $\cos\psi$ is always negative. Near to $\psi = \pi$ the value of $\cos\psi$ reaches a maximum and there is a possibility of observing here emission coming from regions where case (B) is realized; electrons contribute right-handed CP $(-)$. Beyond that region again there is a possibility for case (A) to occur and left-handed CP to be observed $(+)$. That is why the CP changes as $+/-/+$ (Fig. 6). The CP intensity should peak under right-handed CP. In principle, there can be found pulsars having $-/+/-$ transitions. This means that the sight line cuts the emission region of the usual pole (where electrons give the usual left-handed CP) so that $\pi/2 < \psi < 3\pi/2$. In this case again the CP intensity should be higher for right-handed CP.

We saw earlier that different frequencies are generated at different distances R from the star's centre. Explaining the changing sense of CP $+/-/+$, we assume that the regions slightly different in height [cases (A) and (B) correspond to different heights]

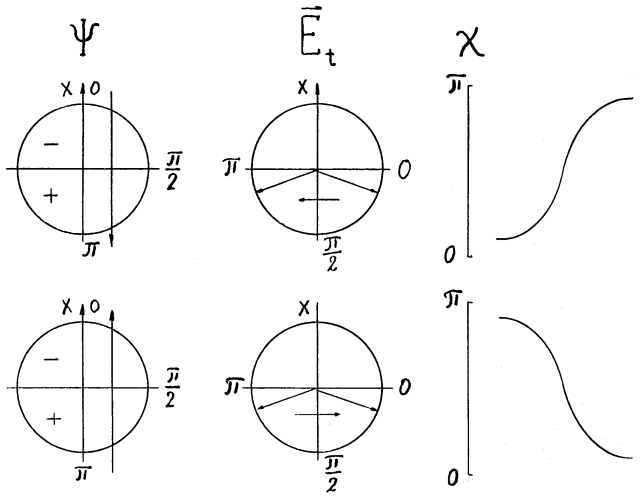

Figure 5. The correlation between variations of PA χ and the antisymmetric CP. The first column shows the sight-line trajectory (solid line). The second column shows the corresponding variations of $\boldsymbol{E}$-vector. The third column represents the corresponding PA variations.

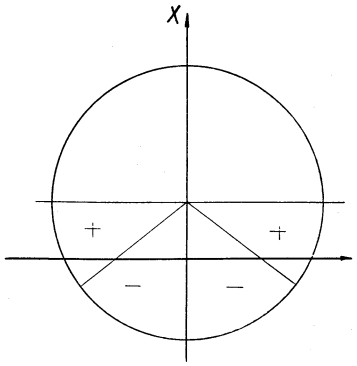

Figure 6. The core-type radiation pattern of the PSR 1541 + 09. The solid line represents the sight-line trajectory. The sectors with + signs represent the regions where the condition (A) is satisfied and the − signs correspond to the regions where case (B) holds.

contribute to the emission diagram at a given frequency. The observations of PSR 1541 + 09 were carried out at frequencies 0.43 and 1.4 GHz (Rankin *et al.* 1989). However, we believe that, if extremely high or low frequencies are observed, this kind of mixture should not occur and the sign change + / − / + will not be observed.

PSR 1702 + 19 has a high degree of CP (60 per cent), indicating that, for most of the emission region cut by the sight line, the condition $\theta^2 < \Delta\gamma k_\varphi c/4\gamma_p^4\omega_B$ is satisfied. This can be understood by assuming that the emission region is elliptical and the sight line cuts it across (along the minor axis). Consequently the pulse width should be narrow. The latter is confirmed by observations.

There is another reason for PSR 1702 − 19 to be an interesting pulsar. The CP of the interpulse has the same handedness as in the main pulse. It is assumed that the main pulse and the interpulse are emitted from regions of different polarity of $\boldsymbol{B}_0$ (Lyne & Manchester 1988). Thus, in case (A) the sign of CP would be different in the main pulse and in the interpulse. In case (B), to keep the sign of CP unchanged both in the main pulse and interpulse, one should cut the emission cone in such a way as to keep the sign of $k_\perp u_\alpha \cos\psi/k_\varphi c$ unchanged (as in Fig. 4b). So, if the sight line cuts the region $-\pi/2 < \psi < \pi/2$ (or $\pi/2 < \psi < 3\pi/2$) in a main pulse, it should cut the region $\pi/2 < \psi < 3\pi/2$ (or $-\pi/2 < \psi < \pi/2$) in the interpulse. The value of $\cos\psi$ reaches a maximum at $\psi = 0, \pi$, so the CP intensity should be maximal at the same place (roughly in the centre of the profile).

5 CONCLUSIONS

We distinguish two types of CP waves. One of them can be composed into two linear orthogonally polarized waves – t and lt. The phase velocities of these waves differ for oblique propagation in a plasma and cannot be coupled into one CP wave. However, on emergence from the plasma, if the phase shift appears to be constant for their further parallel propagation, they will

be perceived as a CP wave. Thus, in the individual pulses, CP can be observed in the profile wings. In fact, the phase shift cannot remain constant even during one pulsar period, due to slight changes of the plasma parameters. Consequently, after summing over many periods the total amount of CP vanishes. Another type of a CP wave is an intrinsically CP wave propagating in a plasma with $\Delta\gamma \neq 0$ at small angles to the magnetic field. The summation gives a net CP. These so-called true CP waves were investigated above. The regularities resulting from our theory are listed below.

(1) The existence of two linearly polarized waves when the sight line cuts the emission diagram far from the diameter, i.e. at large impact parameters (the condition $\theta^2 \equiv k_\perp^2/k_\varphi^2 \gg \Delta\gamma k_\varphi c/4\gamma_p^4\omega_B$ is necessary). In the contrary case, when the sight-line trajectory is close to the centre of the emission diagram (small impact parameter), CP emission should be observed (the condition $\theta^2 \ll \Delta\gamma k_\varphi c/4\gamma_p^4\omega_B$ is necessary). There are no CP waves with large values of θ.

(2) In core-type emission, the CP intensity is greatest and that of linear polarization is lowest (almost zero). In cone-type emission, the opposite is the case.

(3) For linearly polarized emission the transitions from one mode to the orthogonal one take place at the edges of the profile. While in the profile centre, large amounts of unpolarized emission should be present.

(4) The geometry of the emission region for different sight-line trajectories is derived.

(5) Pulsars having symmetric CP at low and high frequencies, and antisymmetric CP at moderate ones are predicted.

(6) Antisymmetric CP $+/-$ is accompanied by decrease of the position angle, while for $-/+$ transitions the PA increases.

(7) The behaviour of the CP in PSR 1542+09 ($+/-/+$) is explained. We suppose that such double transitions of the CP should not occur when the observations are carried out at extremely high or low frequencies. At the transitions of CP ($+/-/+$) in regions with right-handed CP ($-$), the intensity of CP ought to be more than in the '+' regions. In addition, the existence of pulsars with CP changing as $-/+/-$ is predicted.

(8) The high percentage of the CP in PSR 1702−19 is explained by the ellipsoidal nature of the emission cone which is cut along its minor axis. Consequently the pulse width should be narrow. The behaviour of CP in this pulsar is explained.

Note that these conclusions should be regarded as general tendencies and not as strict laws.

ACKNOWLEDGMENTS

We thank J. Rankin for giving us a copy of the paper by Radhakrishnan & Rankin (1990) prior to publication and for most useful discussions. We also thank an anonymous referee for critical notes which improved the paper.

REFERENCES

Allen, M. C. & Melrose, D. B., 1982. *Proc. Astr. Soc. Aust.*, **4,** 365.
Arons, J., 1981. *Proc. Varenna Summer School & Workshop on Plasma Astrophysics,* ESA, p. 273.
Backer, D. C. & Rankin, J. M., 1980. *Astrophys. J.*, **42,** 143.
Beskin, V. S., Gurevich, A. V. & Istomin, Ya.N., 1988. *Astrophys. Space Sci.*, **146,** 205.
Biggs, J. D., Lyne, A. G., Hamilton, P. A., McCulloch, P. M. & Manchester, R. N., 1988. *Mon. Not. R. astr. Soc.*, **235,** 255.
Cheng, A. F. & Ruderman, M. A., 1977. *Astrophys. J.*, **229,** 348.
Ferguson, D. C. & Seiradakis, J. H., 1978. *Astr. Astrophys.*, **64,** 27.
Ginzburg, V. L. & Zheleznyakov, V. V., 1975. *Ann. Rev. Astr. Astrophys.*, **13,** 511.
Goldreich, P. & Julian, W., 1969. *Astrophys. J.*, **157,** 869.
Kazbegi, A. Z., Machabeli, G. Z. & Melikidze, G. I., 1987. *Aust. J. Phys.*, **40,** 755.
Kazbegi, A. Z., Machabeli, G. Z., Melikidze, G. I. & Usov, V. V., 1989a. *Proc. Joint Varenna–Abastumani International School & Workshop on Plasma Astrophysics,* ESA SP-285, Vol. 1, p. 271.
Kazbegi, A. Z., Machabeli, G. Z. & Melikidze, G. I., 1989b. *Proc. Joint Varenna–Abastumani International School & Workshop on Plasma Astrophysics,* ESA SP-285, Vol. 1, p. 277.
Lominadze, J. G., Machabeli, G. Z., Melikidze, G. I. & Pataraya, A. D., 1986. *Sov. J. Plasma Phys.*, **12,** 712.
Lyne, A. G. & Manchester, R. N., 1988. *Mon. Not. R. astr. Soc.*, **234,** 477.
Machabeli, G. Z. & Usov, V. V., 1979. *Sov. Astr. Lett.*, **59,** 1104.
Manchester, R. N. & Taylor, J. H., 1977. *Pulsars,* Freeman, San Francisco.
Radhakrishnan, V. & Rankin, J. M., 1990. *Astrophys. J.*, **352,** 258.
Rankin, J. M., 1983. *Astrophys. J.*, **274,** 333.
Rankin, J. M., 1986. *Astrophys. J.*, **301,** 901.
Rankin, J. M., Stinebring, D. R. & Weisberg, J. M., 1989. *Astrophys. J.*, **346,** 869.
Ruderman, M. A. & Sutherland, P. G., 1975. *Astrophys. J.*, **196,** 51.
Shafranov, V. D., 1967. *Reviews of Plasma Physics,* Vol. 3, Consultants Bureau, New York.
Stinebring, D. R., Cordes, J. M., Rankin, J. M., Weisberg, J. M. & Boriakoff, V., 1984. *Astrophys. J. Suppl.*, **55,** 247.
Sturrock, P. A., 1971. *Astrophys. J.*, **164,** 529.
Taylor, J. H. & Stinebring, D. R., 1986. *Ann. Rev. Astr. Astrophys.*, **24,** 285.
Volokitin, A. S., Krasnoselskikh, V. V. & Machabeli, G. Z., 1985. *Sov. J. Plasma Phys.*, **11,** 310.